

## Unifying Model for Several Classes of Two-Dimensional Phase Transition

Yonatan Dubi,<sup>1</sup> Yigal Meir,<sup>1,2</sup> and Yshai Avishai<sup>1,2</sup>

<sup>1</sup>*Physics Department, Ben-Gurion University, Beer Sheva 84105, Israel*

<sup>2</sup>*The Ilse Katz Center for Meso- and Nano-scale Science and Technology, Ben-Gurion University, Beer Sheva 84105, Israel*

(Received 29 September 2004; published 22 April 2005)

A relatively simple and physically transparent model based on quantum percolation and dephasing is employed to construct a global phase diagram which encodes and unifies the critical physics of the quantum Hall, “two-dimensional metal-insulator,” classical percolation and, to some extent, superconductor-insulator transitions. Using real-space renormalization group techniques, crossover functions between critical points are calculated. The critical behavior around each fixed point is analyzed and some experimentally relevant puzzles are addressed.

DOI: 10.1103/PhysRevLett.94.156406

PACS numbers: 71.30.+h, 73.43.Nq, 74.20.Mn

Two-dimensional phase transitions have been a focus of interest for many years, as they may be the paradigms of second order quantum phase transitions (QPTs). However, in spite of the abundance of experimental and theoretical information, there are still unresolved issues concerning the behavior of some of these transitions at and near criticality, most simply exposed by the value of the critical exponent  $\nu$  (describing the divergence of the correlation length at the transition). Below we discuss three examples which underscore these problems. First, in the integer quantum Hall (QH) effect, which is usually described within the single particle framework, various numerical studies yielded a critical exponent  $\nu \approx 2.35$  [1], in agreement with heuristic arguments [2]. Some experiments indeed reported values around 2.4 [3], while others reported exponents around 1.3 [4], close to the classical percolation exponent  $\nu_p = 4/3$ . Even more perplexing, some experiments claim that the width of the transition does not shrink to zero at vanishing temperature [5], in contradiction with the concept of a QPT. Additionally, the observation of a QH insulator [6] is inconsistent with the QPT scenario [7]. Consider secondly the superconductor (SC) insulator transition (SIT), for which theoretical studies suggest several scenarios. Similar to the QH situation, some experiments yield a value  $\nu \approx 1.3$  [8], not far from the value  $\nu \approx 1$ , predicted by numerical simulations within the random boson model, but closer to the classical percolation value. Other experiments, however, yield  $\nu \approx 2.8$  [9], while some experiments claim an intermediate metallic phase [10]. As a third example, consider the recently claimed metal-insulator transition (MIT) [11]. The critical exponent is again close to 1.3 [12,13] but the occurrence of such phase transition is in clear contrast with the scaling theory of localization.

The basic question which naturally arises is then whether it is possible to unify these phase transitions within a single theory and thereby resolve some of the problems raised above. A hint toward an affirmative answer is gained by experimental indications that percolation plays a key role in both the QH transition [14] and in the SIT [15]. Moreover, its relevance to the MIT has been

argued theoretically and observed experimentally [12,13,16]. The QH and the SIT have been treated within a percolationlike model in Ref. [17], consisting of SC or QH droplets connected via quantum tunneling, similar in spirit to the model presented in [18].

In the present work we address these issues using a physically transparent picture. This formalism is a generalization of an approach which proved to be quite successful for describing the QH transition and some aspects of the SIT [18]. Introducing decoherence into the model, we are able to include the QH transition (or the SIT), classical percolation, and the MIT all within the same phase diagram. Employing real-space renormalization group (RSRG) techniques, we calculate the critical exponents, analyze this phase diagram to understand the possible critical behaviors, and expose the physical conditions necessary to observe them. The crossover between different critical points, which may be explored experimentally, is investigated and concrete experimental predictions are made.

For the sake of completeness, the model used to describe the QH effect [18] is briefly explained here. In strong magnetic fields, electrons with Fermi energy  $\epsilon_F$  perform small oscillations around equipotential lines. When  $\epsilon_F$  is small, their trajectories are trapped inside potential valleys, with weak tunneling occurring between adjacent valleys. We associate each such potential valley with a site in a lattice. Nearest neighbor valleys (localized orbits) are connected by links representing quantum tunneling between them. As  $\epsilon_F$  increases and crosses the saddle-point energy separating two neighboring valleys, the two isolated trajectories coalesce; the electron can freely move from one valley to its neighbor and the link connecting them becomes perfect (or SC). The QH transition occurs when an electron can traverse the sample along an equipotential trajectory (an edge state), which in the model occurs when a cluster of SC links connects the two sides of the system (a percolating cluster). Consequently, the QH problem maps onto a mixture of SC and quantum links on a lattice. Each link carries a left-going and a right-going channel. In accordance with the physics at strong magnetic fields there is no scattering in the junctions (valleys) and

the edge state continues propagating uninterrupted according to its chirality, while the scattering occurs on the link (saddle point) itself. Each scatterer is characterized by its scattering matrix  $S_i$ , namely, a transmission probability  $T_i$  and phases. The critical behavior of the QH transition is encoded by the scaling behavior near the SC percolation point of this lattice model. Calculation of the transmission through such a system, using two different numerical approaches, yielded a diverging localization length, with an exponent  $\nu \approx 2.4 \pm 0.1$ , close to the results of other numerical estimates [1]. Importantly, as pointed out in [18], this model, unlike other models describing the QH transition—such as the Chalker-Coddington model [19]—has two diverging length scales: the localization length and the percolation coherence length.

An important feature, which may be very relevant to the experimental observations, is dephasing. In order to incorporate it into the above model, a fraction of the links is attached to current-conserving phase-disrupting reservoirs [20]. An electron propagating along such a link enters the reservoir and it, or another electron, emerges from it with a random phase (there is no net current into the reservoir). Transport along this link is therefore incoherent. The lattice now consists of three types of links [Fig. 1(a)]: a fraction  $p$  of SC links (i.e., quantum links whose transmission is unity), a fraction  $q$  of classical, or incoherent links, and fraction  $1 - p - q$  of quantum tunneling links. The principal objective is then to construct a phase diagram in the  $(p, q)$  plane of parameters and to identify the various critical transitions.

For simplicity we will study the model on a square lattice, and our main tool will be the RSRG scheme. Rescaling the lattice by a factor of 2, each  $2 \times 2$  square is mapped onto a  $1 \times 1$  square [Fig. 1(b)]. Each link is characterized by a scattering matrix and whether or not it is connected to a phase-breaking reservoir. Given the information for each link, the transmission through the whole unit is evaluated by attaching leads to its left and right sides (see below). This enables us to follow the distribution of the transmission amplitudes, and the fraction of incoherent links, from one iteration to another, and eventually evaluate the distribution for the entire lattice. For the classical problem, this calculation reduces to the evaluation of transport through a Wheatstone bridge, where the symmetry of the square lattice has been used. For simplicity we use the same geometry for the quantum problem [Fig. 1(c)], and later verify that the addition of dangling bonds does not modify the critical behavior.

Let us first demonstrate the process for  $q = 0$ , which reduces to our previous, fully coherent model. For each realization of disorder, i.e., the scattering matrices on the 5 links, each determined by transmission probability  $T_i$  and phases, we can evaluate exactly the transmission probability through the Wheatstone bridge,  $\hat{T}(\{T_i\}, \phi)$ , where  $\phi$  stands for all the independent phases, and thus follow its distribution from one iteration to another, allowing us to

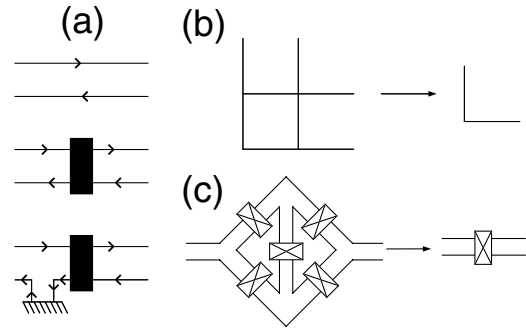


FIG. 1. (a) The three possible links: a superconducting link (top), where the transmission along the link is unity; a quantum link (middle), where the transmission is determined by a random scattering matrix; and an incoherent link (bottom), where the electron phase is randomized by a current-conserving reservoir. In the calculations such reservoirs were attached to all 4 sides of the scatterer. (b) The mapping of a  $2 \times 2$  square onto a  $1 \times 1$  square, resulting in reducing the lattice size by a factor of 2. (c) The RG calculation for the Wheatstone bridge. Each link is one of the three possibilities depicted in (a), with initial probabilities  $p$ ,  $1 - p - q$ , and  $q$ , respectively. The transmission through the equivalent link is evaluated, and determines the nature of the link and its parameters for the next iteration.

determine the fixed points and the RSRG flow. If one starts with a distribution of scattering matrices whose phases are uniformly distributed, they remain so, and thus we will be interested only in the scaling of the distribution of the transmission probabilities,

$$G^{\{n\}}(T) = \int \dots \int \delta[T - \hat{T}(T_1, \dots, T_5, \phi)] \times G^{\{n-1\}}(T_1) \dots G^{\{n-1\}}(T_5) dT_1 \dots dT_5 d\phi. \quad (1)$$

The initial distribution can be written as

$$G^{\{0\}}(T) = p\delta(T - 1) + (1 - p)\hat{G}^{\{0\}}(T), \quad (2)$$

where  $p$  is the fraction of SC links (namely, the fraction of saddle-point energies that are below the Fermi energy).  $\hat{G}^{\{0\}}(T)$  is determined by the dependence of the transmission on energy and by distribution of the saddle-point energies. However, the initial distribution  $\hat{G}^{\{0\}}(T)$  does not affect the critical behavior, as the distribution always flows toward one of three possible fixed-point distributions.

Since the probability that the transmission is unity is determined by the classical percolation probability, one finds

$$G^{\{n\}}(T) = P_n(p)\delta(T - 1) + (1 - P_n(p))\hat{G}^{\{n\}}(T, p), \quad (3)$$

where  $P_n(p)$  is the classical percolation probability after  $n$  iterations, and  $\hat{G}^{\{n\}}$  can be exactly expressed in terms of  $\hat{G}^{\{n-1\}}$ . Clearly, if  $p < p_c$ ,  $P(p)$  flows toward zero, while for  $p > p_c$  it flows to unity. At  $p = p_c$  the distribution  $\hat{G}$  flows toward a two-peak fixed distribution, similar to pre-

viously obtained results for the QH transition [21]. The critical behavior can be deduced by investigating the length dependence of the averaged transmission near the critical point and its collapse using  $T(p, L) = T[L/\xi(p)]$ , where  $\xi(p)$  is an energy (or concentration) dependent localization length. We find that  $\xi(p)$  diverges at  $p_c = 1/2$  with an exponent  $\nu = 2.4 \pm 0.1$ , consistent with previous numerical calculations for the QH transition [1].

Having demonstrated the power of the RSRG technique for  $q = 0$  (no dephasing) we now treat the model at an arbitrary point  $(p, q)$ . Qualitatively, several phase transitions can be identified. For  $q = 0$  the QH transition is recovered as demonstrated above. For  $p + q = 1$  (no quantum links) the point  $q = p_c = \frac{1}{2}$  describes the classical conductor-superconductor percolation transition. For the case of  $p = 0$ , all the links are either quantum (with  $T < 1$ ) or classical. This is the model suggested in Refs. [12,16] to describe the ‘‘apparent’’ metal-insulator transition in two dimensions. The flow lines can be determined without the full quantum calculations by noticing that the rescaled cell will be SC if a cluster of SC links percolate, while it will be an incoherent metal if there is percolation of classical links, and no percolation of SC ones. These conditions define the RSRG equations for the quantities  $p$  and  $q$ ,

$$\begin{aligned} p' &= 2(1-p)^3 p^2 + 8(1-p)^2 p^3 + 5(1-p)p^4 + p^5 \\ q' &= q\{10p^4 - 20p^3(1-q) + 2p(1-q)[2 + 5(1-q)q] \\ &\quad + q(2 + 2q - 5q^2 + 2q^3) + 2p(2 + 3q - 10q^2 + 5q^3)\}. \end{aligned} \quad (4)$$

The full phase diagram thus contains three limiting phases: an Anderson insulator, a superconductor (or a QH phase), and an incoherent metal, and is depicted in Fig. 2. The fact that for  $p > \frac{1}{2}$  one gets a QH phase is easily understandable, as once there is percolation of SC links there is an edge state propagating without backscattering through the system. The transition between an Anderson insulator and an incoherent metal is more intriguing. Once  $p + q > \frac{1}{2}$  an electron can propagate freely from one side of the system to the other, but necessarily undergoes an incoherent scattering event, and thus this phase is an incoherent metal. For  $p + q < \frac{1}{2}$ , however, there is no trajectory that allows the electron to traverse the system without quantum tunneling. These tunneling events, however, are intertwined with incoherent scattering, and thus the conductance of the system will be of the order of  $\exp(-L_\phi/\xi)$ , where  $L_\phi \sim q^{-1/2\phi}$  is the average distance between incoherent scattering events. As  $q$  decreases, the conductance of the system goes to zero, ending up as an Anderson insulator. For finite  $p$ , however, the existence of incoherent scattering is not expected to affect the quantization of the Hall conductance [22]. Thus one may characterize the phase with finite  $p$  and  $q$ , but with  $p + q < \frac{1}{2}$  as a ‘‘Hall insulator.’’ In agreement with previous treatments of this phase, we also conclude that it only exists for finite de-

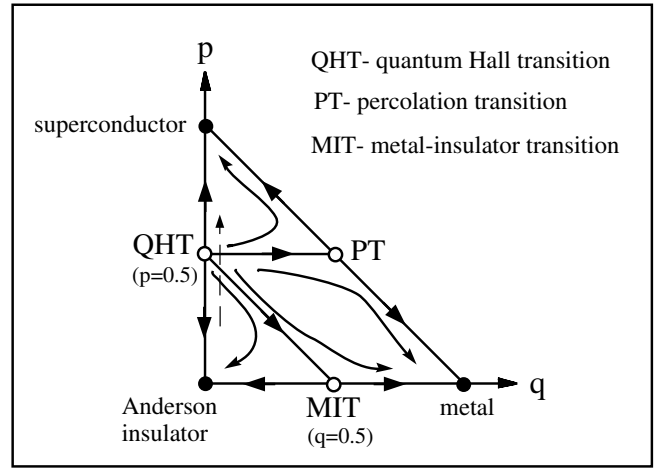


FIG. 2. The phase diagram of the model in term of the parameters  $p$ , the concentration of a perfect-transmission link, and  $q$ , the probability of incoherent links. The phase diagram displays three different phase transitions between the three different phases. The broken line represents a possible experimental trajectory leading to a finite metallic phase.

phasing ( $q > 0$ ), as for  $q = 0$  the system flows to an Anderson insulator. Further investigation of this phase will be reported elsewhere.

Beyond the characterization of the different phases, the model allows a direct calculation of the crossover between them. RSRG on the line  $p = \frac{1}{2}$  allows, as a function of  $q$ , to study the crossover between the quantum SIT (or the QH transition) to the classical superconductor-conductor transition. Following the RSRG flow along this line, we find that the average transmission obeys

$$T\left(q, p = \frac{1}{2}\right) = T_0 \left[ 1 + \beta \left( \frac{L}{L_\phi(q)} \right)^{0.91} \right], \quad (5)$$

with  $L_\phi(q)$  defined above and  $\beta$  some nonuniversal constant. This function correctly reproduces the two fixed-point behaviors,  $T = T_0$  at the QH transition and  $T \sim L^{t/\nu_p}$  at the classical percolation critical point. The values of  $t$ , the resistance critical exponent, and  $\nu_p$  obtained separately by RSRG are 1.33 and 1.42, respectively, giving  $t/\nu_p \sim 0.93$ , in good agreement with the limiting behavior of the crossover function (5). The effect of incoherent scattering on the critical behavior may explain the different critical exponents observed in QH and in SITs, which mostly agree with one of the critical exponents associated with these two critical points.

The QH to the MIT crossover has been demonstrated experimentally [23]. The present formalism allows us to study this crossover theoretically, by following the conductance along the line  $p + q = \frac{1}{2}$ . The dependence of the transmission on length for different values of  $q$  along this line is depicted in Fig. 3. There is a clear crossover from a constant (QH behavior) to  $T \sim L^{t/\nu_p}$  (classical behavior) as before. The length scale determining this crossover (see

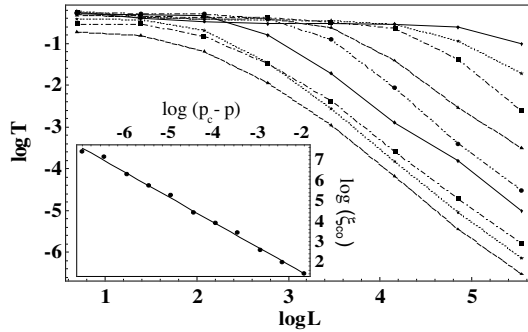


FIG. 3. Crossover from the QH critical point to the MIT: transmission as a function of length (on a log-log scale) for different values of  $(p_c - p)$ , demonstrating the crossover from the QH behavior (length-independent transmission) to a classical power-law dependence. Inset: the crossover length  $\xi_{co}$  as a function of the  $(p_c - p)$  on a log-log scale, with a slope  $\nu = 1.23$ , close to the percolation correlation exponent.

inset of Fig. 3) is found to be the percolation correlation length; namely, for  $L < \xi_p$  the system behaves quantum mechanically, and classically for  $L > \xi_p$ .

All these observations have clear experimental relevance. As mentioned above, the QH to the MIT crossover has been investigated experimentally, but with no detailed investigation of the critical behavior. We thus predict that the critical exponent along this line will be the classical percolation exponent,  $\nu_p$ , and not the QH exponent, with two relevant length scales for any finite system. Similarly, one can experimentally investigate the quantum SIT to the classical superconductor-conductor transition, for different temperatures. The theory predicts that once the dephasing length becomes smaller than the system size (i.e.,  $q$  becomes nonzero), the critical behavior will correspond to classical percolation. Moreover, we predict that the conductance at the critical point will vary from its universal value at the quantum transition, as observed experimentally [24] by a length dependent value according to Eq. (5).

Another result of the proposed phase diagram is the existence of an intermediate metallic regime in the QH and in the SITs. Imagine changing a physical parameter (e.g., density or magnetic field) along the broken line in Fig. 2. Then there is one transition from an insulator to an incoherent metal, and then from a metal to a QH liquid (or a superconductor), consistent with experimental observations for the QH transition [5] and the SIT [10]. The critical behavior of both of these transitions is determined by classical percolation. Thus the theory predicts that the QH critical behavior can only be observed in system where these transitions coalesce into a single transition. This can be tuned, for example, by lowering the temperature and changing the dephasing length. Thus the theory can explain the different exponents observed experimentally and predicts a crossover between the different critical behaviors as a function of temperature.

It should be noted that some aspects of this phase diagram are not dissimilar to the one presented in Ref. [25]. Here, however, we do not invoke any zero temperature dissipation. Rather, if, as expected, the dephasing length diverges at  $T \rightarrow 0$  (i.e.,  $q \rightarrow 0$ ), the theory predicts only two stable phases: the QH (or superconducting) phase and the Anderson insulator phase.

We would like to acknowledge fruitful discussions with A. Aharony and O. Entin-Wohlman. This research has been funded by the ISF.

- 
- [1] B. Huckestein, Rev. Mod. Phys. **67**, 357 (1995).
  - [2] C. V. Mil'nikov and I. M. Sokolov, JETP Lett. **48**, 536 (1988).
  - [3] H. P. Wei *et al.*, Phys. Rev. Lett. **61**, 1294 (1988); S. Koch *et al.*, Phys. Rev. Lett. **67**, 883 (1991).
  - [4] A. A. Shashkin *et al.*, Phys. Rev. B **49**, 14486 (1994); R. B. Dunford *et al.*, Physica B (Amsterdam), **298**, 496 (2001).
  - [5] D. Shahar *et al.*, Solid State Commun. **107**, 19 (1998); N. Q. Balaban *et al.*, Phys. Rev. Lett. **81**, 4967 (1998).
  - [6] P. Hopkins *et al.*, Phys. Rev. B **39**, 12708 (1989); M. Hilke *et al.*, Nature (London) **395**, 675 (1998).
  - [7] L. P. Pryadko and A. Auerbach, Phys. Rev. Lett. **82**, 1253 (1999).
  - [8] D. B. Haviland, Y. Liu, and A. M. Goldman, Phys. Rev. Lett. **62**, 2180 (1989).
  - [9] Y. Liu *et al.*, Phys. Rev. Lett. **67**, 2068 (1991).
  - [10] A. F. Hebard and M. A. Paalanen, Phys. Rev. Lett. **65**, 927 (1990); A. Yazdani and A. Kapitulnik, Phys. Rev. Lett. **74**, 3037 (1995); D. Ephron *et al.*, Phys. Rev. Lett. **76**, 1529 (1996); N. Mason and A. Kapitulnik, Phys. Rev. Lett. **82**, 5341 (1999).
  - [11] E. Abrahams, S. V. Kravchenko, and M. P. Sarachik, Rev. Mod. Phys. **73**, 251 (2001) and references therein.
  - [12] Y. Meir, Phys. Rev. Lett. **83**, 3506 (1999), and experimental references therein.
  - [13] S. Das Sarma *et al.*, cond-mat/0406655.
  - [14] A. A. Shashkin *et al.*, Phys. Rev. Lett. **73**, 3141 (1994); I. V. Kukushkin *et al.*, Phys. Rev. B **53**, R13260 (1996).
  - [15] D. Kowal and Z. Ovadyahu, Solid State Commun. **90**, 783 (1994).
  - [16] S. He and X. C. Xie, Phys. Rev. Lett. **80**, 3324 (1998).
  - [17] E. Shmishoni, A. Auerbach, and A. Kapitulnik, Phys. Rev. Lett. **80**, 3352 (1998).
  - [18] Y. Dubi, Y. Meir, and Y. Avishai, Phys. Rev. B **71**, 125311 (2005).
  - [19] J. T. Chalker and P. D. Coddington, J. Phys. C **21**, 2665 (1988).
  - [20] M. Buttiker, Phys. Rev. B **33**, 3020 (1986); see also J. Shi, S. He, and X. C. Xie, cond-mat/9904393.
  - [21] D. P. Arovas, M. Janssen, and B. Shapiro, Phys. Rev. B **56**, 4751 (1997); A. G. Galstyan and M. E. Raikh, Phys. Rev. B **56**, 1422 (1997); Y. Avishai, Y. Band, and D. Brown, Phys. Rev. B **60**, 8992 (1999).
  - [22] E. Shmishoni, cond-mat/0406703.
  - [23] Y. Hanein *et al.*, Nature (London) **400**, 735 (1999).
  - [24] Y. Liu *et al.*, Phys. Rev. B **47**, 5931 (1993).
  - [25] A. Kapitulnik *et al.*, Phys. Rev. B **63**, 125322 (2001).